Materials Research Bulletin 74 (2016) 78–84

Contents lists available at ScienceDirect

Materials Research Bulletin

journal homepage: www.elsevier.com/locate/matresbu

Comprehensive studies of structural, electronic and magnetic properties of $Zn_{0.95}Co_{0.05}O$ nanopowders

Ivana Radisavljević[a,*], Nikola Novaković[a], Branko Matović[a], Novica Paunović[b], Mirjana Medić[a], Nenad Bundaleski[a,c], Velibor Andrić[a], Orlando M.N.D. Teodoro[c]

[a] University of Belgrade—Vinča Institute of Nuclear Sciences, P.O. Box 522, 11001 Belgrade, Serbia
[b] University of Belgrade—Institute of Physics, Pregrevica 118, 11000 Belgrade, Serbia
[c] Universidade Nova de Lisboa—Faculdade de Ciências e Tecnologia, Quinta da Torre 2829-516 Caparica, Portugal

ARTICLE INFO

Article history:
Received 8 May 2015
Received in revised form 22 September 2015
Accepted 6 October 2015
Available online 18 October 2015

Keywords:
A. Semiconductors
A. Oxides
B. Magnetic properties
C. XAFS
D. Electronic structure

ABSTRACT

X-ray absorption (XANES, EXAFS, XMCD) and photoelectron (XPS) spectroscopic techniques were employed to study local structural, electronic and magnetic properties of $Zn_{0.95}Co_{0.05}O$ nanopowders. The substitutional Co^{2+} ions are incorporated in ZnO lattice at regular Zn sites and the sample is characterized by high structural order. There was no sign of ferromagnetic ordering of Co magnetic moments and the sample is in paramagnetic state at all temperatures down to 5 K. The possible connection of the structural defects with the absence of ferromagnetism is discussed on the basis of theoretical calculations of the O K-edge absorption spectra.

1. Introduction

Diluted magnetic semiconductors (DMS) continue to attract scientific attention both from theoretical and experimental point of view due to their unique properties that will eventually enable to simultaneously manipulate both spin and charge of the electrons. Typical DMS materials of the type II–VI and III–V (e.g., transition metal (TM)-doped InAs, GaAs, ZnTe and CdTe) even if magnetically ordered, have the Curie temperatures (T_C) below room temperature, which makes them less attractive for practical applications. ZnO is a promising host DMS material envisaged to exhibit room temperature ferromagnetism (RTFM) when doped with most of the TM elements [1]. However, there exists a great deal of controversy regarding the origins and nature of the observed magnetic response, even for the most extensively studied Co-doped ZnO. Although many experimental reports ascertain its intrinsic ferromagnetism (FM) [2–8], some found that Co 3d-electrons are not directly at the origin of the FM response [9]. To account for the observed RTFM in $Zn_{1-x}Co_xO$ with a paramagnetic Co sublattice, the research attention focused on resolving the role played by structural defects in inducing and mediating magnetism, which would soon become another highly controversial issue, especially upon discovery that the host ZnO material itself can be magnetic even without transition-metal doping [10–14]. Many authors believe that stabilization of the FM interaction relies on the presence of oxygen vacancies (O_v) [15,16]. Others claim that an oxygen vacancy by itself would not cause ferromagnetism [17] and that actually zinc interstitials (Zn_i) play a crucial role in mediating FM interaction [18]. According to [3] intrinsic defects suppress magnetism, while according to [19,20] appreciable FM response requires Co interstitials (Co_i) which would directly interact with substitutional Co atoms. The latter is in disagreement with presumable connection between the uniformity of Co ions distribution and inherent FM of $Zn_{1-x}Co_xO$ [3,21]. The existence of Co-enriched zones in the ZnO matrix is expected to favour antiferromagnetic (AFM) interaction between Co ions due to their small separation distance [19,22–25]. To mediate the FM coupling between unpaired Co electrons, co-doping with impurities such as H [26,27], Ga [28], Cu [29,30], Gd [31] and Li [32] is proposed. Recently an increasing number of experimental reports provide evidence for intrinsic paramagnetism (PM) of Co-doped ZnO [19,33–39]. These findings are supported by theoretical calculations which predict the PM ground state of Co-doped ZnO at RT as a result of weak Co–Co coupling [40,41].

Inconsistencies in the experimental findings on Co-doped ZnO magnetic properties and their correlation with the local and electronic structure urge for even more comprehensive investigations. This paper presents detailed analysis of the structural,

* Corresponding author. Fax: +381 11 3440 100.
E-mail address: iva@vin.bg.ac.rs (I. Radisavljević).

http://dx.doi.org/10.1016/j.materresbull.2015.10.014
0025-5408/

electronic and magnetic properties of the $Zn_{0.95}Co_{0.05}O$ nanopowders. X-ray absorption near edge structure (XANES), x-ray absorption fine structure (EXAFS), x-ray photoelectron spectroscopy (XPS) and x-ray magnetic circular dichroism (XMCD) were employed to study the local electronic and magnetic structure of Co and O. Compositional, structural and magnetic properties were studied by inductively-coupled plasma optical emission spectrometry (ICP-OES), x-ray diffraction (XRD), x-ray fluorescence (XRF) and vibrating sample magnetometry (VSM). To examine the presence of intrinsic defects (vacancies and interstitials) in the investigated sample and their possible connection to magnetism, theoretical calculations of the O K-edge absorption spectra were performed.

2. Experiment and theoretical calculation

Glycine–nitrate method was applied to synthesize ZnO solid solutions doped with nominal concentration of 5 at.% Co. Zn–nitrate hexahydrate, Co–nitrate hexahydrate and aminoacteic acid-glycine (Alfa Aesar GmbH, Germany) were dissolved with small amount of distilled water according to desired composition of the final solid solution powder. Stainless steel beaker was used as a reactor. The solution was heated in a muffle furnace until the burn-up process terminated (about 450 °C). The obtained ash powder was afterward calcined at 600 °C for 4 h. X-ray diffraction (XRD) measurements were performed on Siemens D5000 diffractometer with Ni filtered Cu-K$\alpha_{1,2}$ radiation in Bragg–Brentano geometry, in the range of angles $10^\circ < 2\theta < 90^\circ$ using a step width 0.02° and acquisition time 2 s/step. Angular correction by high quality Si standard is done prior to the measurements. Composition of the sample is checked using inductively-coupled plasma optical emission spectrometry. Sample was digested using microwave assisted technique with Milestone Ethos-1 instrument according to Digestion application note DG-ME-32. Specific amount of the sample (0.25 g) was transferred in a teflon vessel and mixed with HNO_3 (7 ml) and HF (1 ml). Closed sample vessel is then treated with microwaves for 30 min at the temperature 220 °C. Solution with digested sample was transferred in volumetric flask and analyzed on ICP-OES PerkinElmer 5000 apparatus.

Energy dispersive X-ray fluorescence (EDXRF) spectroscopy was performed using EDXRF Camberra spectrometer with Rh excitation source (800 μA, 40 kV, exposure time 180 s).

Magnetic properties were measured with a vibrating sample magnetometer VSM 2000 in the temperature range between 5 K and room temperature (RT). Zero-field cooled/field cooled (ZFC/FC) measurements were performed in the following manner. First at zero field ($B = 0$) the sample was cooled down from RT to 5 K, then the field ($B = 5$, 15 and 50 mT) was applied and the measurements were performed while warming up from 5 K to RT in the field. FC measurements were performed immediately after ZFC measurement while cooling down the sample from RT to 5 K under the applied field ($B = 5$, 15, 50 mT).

EXAFS/XANES measurements on Co K-edge were performed in the fluorescence mode at 8 K and RT on the HASYLAB C1 Beamline at Deutsches Elektronen-Synchrotron DESY (Hamburg, Germany). Data processing and analysis were performed using IFEFFIT [42] as implemented in ATHENA and ARTEMIS software packages [43]. XANES/XMCD measurements on Co $L_{2,3}$- and O K-edge were performed in the total-electron yield (TEY) mode at 4 K and RT on the Circular Polarization Beamline at Elettra Synchrotron Radiation Facility (Trieste, Italy). To measure circularly polarized absorption spectra, external magnetic field $B = 0.3$ T was applied perpendicular to the sample surface and photon helicity ρ^+ (right-handed) and ρ^- (left-handed) was reversed at each photon energy. The degree of circular polarization was 80% and the energy resolution 0.6 eV.

XPS measurements were performed on a VSW XPS system and the Class 100 energy analyzer being a part of an experimental setup assembled for surface investigation [44]. The powdered sample was pressed onto an indium foil in order to provide mechanical support and electrical contact. The spectra were taken on as-

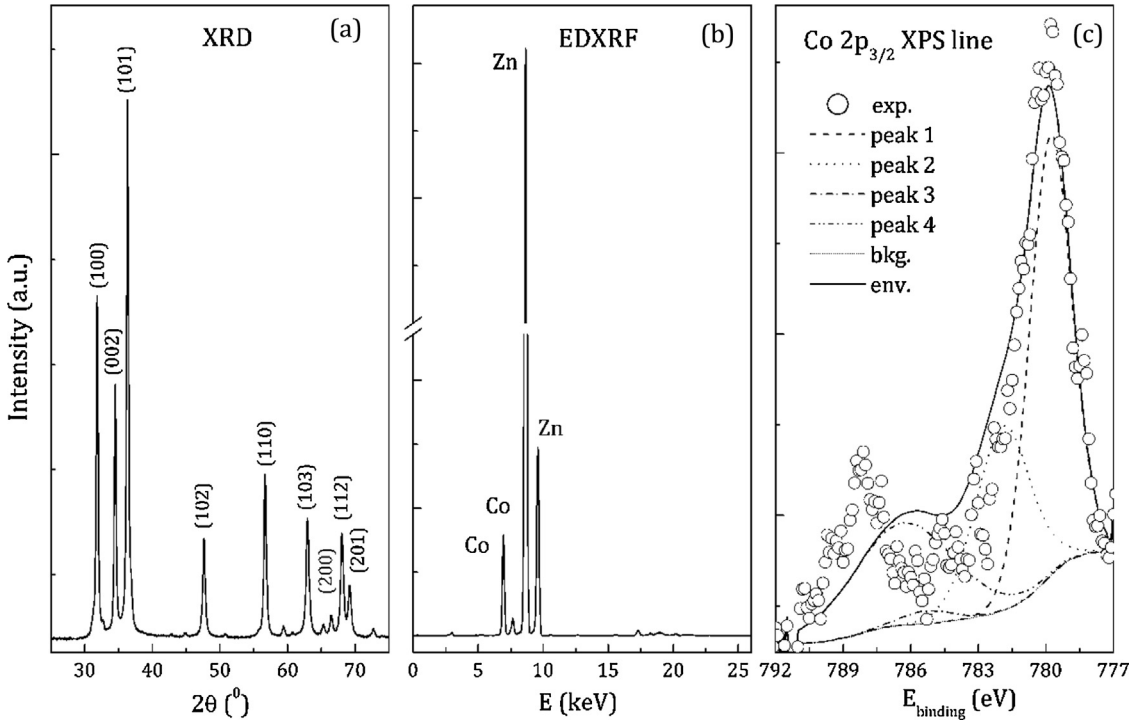

Fig. 1. (a) XRD spectrum and (b) EDXRF spectrum of $Zn_{0.95}Co_{0.05}O$; (c) Experimental Co $2p_{3/2}$ XPS spectrum (open circles) and the fit. The fine multiplet structure of the main Co $2p_{3/2}$ XPS line (at ≈780 eV) and its satellite (at ≈788 eV) can be resolved into four components represented with broken lines (see text for more details). Background (bkg) and envelope (env) functions are represented with full lines.

received sample using non-monochromatic Mg–Kα line (1256.3 eV). The energy axis was calibrated using the Ag-$3d_{5/2}$ XPS line position (368.22 eV) of sputter-cleaned Ag (110) monocrystal and the Au-$4f_{7/2}$ XPS line position (83.96 eV) of sputter-cleaned polycrystalline Au sample. The effect of charging had negligible influence on the energy spectra.

Theoretical modelling of the O K-edge XANES spectra were performed using real space full multiple scattering FEFF 9.03 code [45] on a cluster containing 259 atoms. Self consistent field approach (SCF) with Hedin–Lundqvist exchange-correlation is used to calculate scattering potentials. To reduce effects of potential discontinuities at the muffin–tin spheres automatic overlapping (AFOLP) is included. The effects of screening of the x-ray field and the photoelectron-core hole interaction were neglected. Program ATOMS [46] is used to generate input files containing different point defects (vacancies/interstitials) around the central O. To account for the finite core–hole life-time and the experimental resolution theoretical XANES spectra were convoluted with 0.1 eV Lorentzian and 0.4 eV Gaussian broadening, respectively.

3. Results and discussion

The XRD pattern of $Zn_{0.95}Co_{0.05}O$ shown in Fig. 1a reveals that the investigated sample has pure wurtzite-type structure (space group $P6_3mc$). The peaks are indexed with their diffraction planes. The obtained lattice parameters $a = b = 3.248$ Å and $c = 5.203$ Å are very close to that of pure ZnO ($a = 3.249$ Å, $c = 5.206$ Å [47]). There was no indication of the presence of impurities and/or secondary impurity phases, within detection limit of XRD and EDXRF measurements (see Fig. 1b). The mass fraction of constitutive elements obtained by ICP-OES compositional analysis (74.97 wt.% Zn, 2.95 wt.% Co and 22.08 wt.% O), within experimental uncertainty (≈10%), corresponds to the nominal composition of the sample (76.63 wt.% Zn, 3.64 wt.% Co and 19.74 wt.% O).

Experimental Co $2p_{3/2}$ XPS spectrum and its fit are presented in Fig. 1c. The broad (non-symmetrical) peak shape of the Co $2p_{3/2}$ XPS spectrum results from the multiplet splitting (i.e., a number of final states created via coupling between the unpaired Co d-electrons in the core with the unpaired outer shell electrons) [48]. The main Co $2p_{3/2}$ XPS line is positioned at ≈780 eV, which corresponds to Co^{2+} oxidation state. Intensive satellite peak at ≈788 eV which accompanies the main XPS line, is characteristic for transition metal monoxides [49]. To account for the fine multiplet structure of the Co $2p_{3/2}$ XPS spectrum, the CoO model [48] is applied, using the same constraints for the number of components (peaks 1–4, see Fig. 2b) and the fitting parameters (intensities and widths of the peaks). The CoO model fairly well describes the experimental spectrum, which implies that Co ions in investigated sample are surrounded by oxygen atoms. The discrepancy between experiment and fit in the region of the satellite peak (785–792 eV) probably originates from the relatively intensive Auger O_{KLL} line [50] superimposed to the main Co $2p_{3/2}$ XPS line. The fit using the constraints for Co_3O_4 and $Co(OH)_2$ yields significantly larger discrepancy from the experiment.

Data collection of the integral magnetic properties is presented in Fig. 2. After subtraction of the linear PM background, magnetization curve M(B) taken at RT (Fig. 2a) reveals a weak FM response. The order of magnitude of the saturation magnetization ($M_{sat} = 0.0015$ emu/g) is comparable to defect induced magnetization (DIM) in pure ZnO [10]. The M(B) curves taken in the temperature range 5–15 K (Fig. 2b) all have closed hysteresis loops with negligible coercivity and low saturation magnetization ($M_{sat} \approx 4$ emu/g). Magnetization curves measured in zero field cooled (ZFC) and field cooled (FC) regimes (Fig. 3c) show no bifurcation characteristic for superparamagnetic (SPM) ordering.

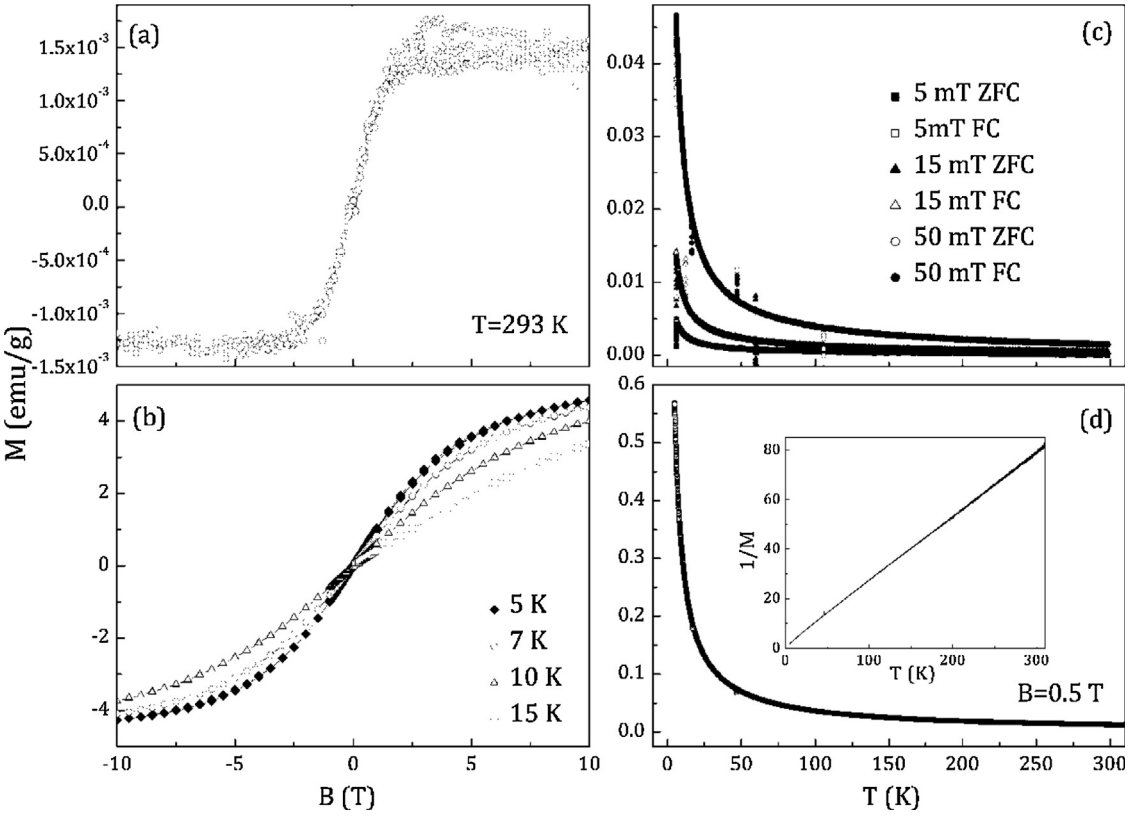

Fig. 2. (a) M(B) curves taken at RT and (b) in the temperature range 5–15 K; (c) ZFC/FC curves measured in the field $B = 5$, 15 and 50 mT; (d) M(T) curve taken at $B = 0.5$ T. Inverse magnetization (1/M) as a function of temperature is shown in inset.

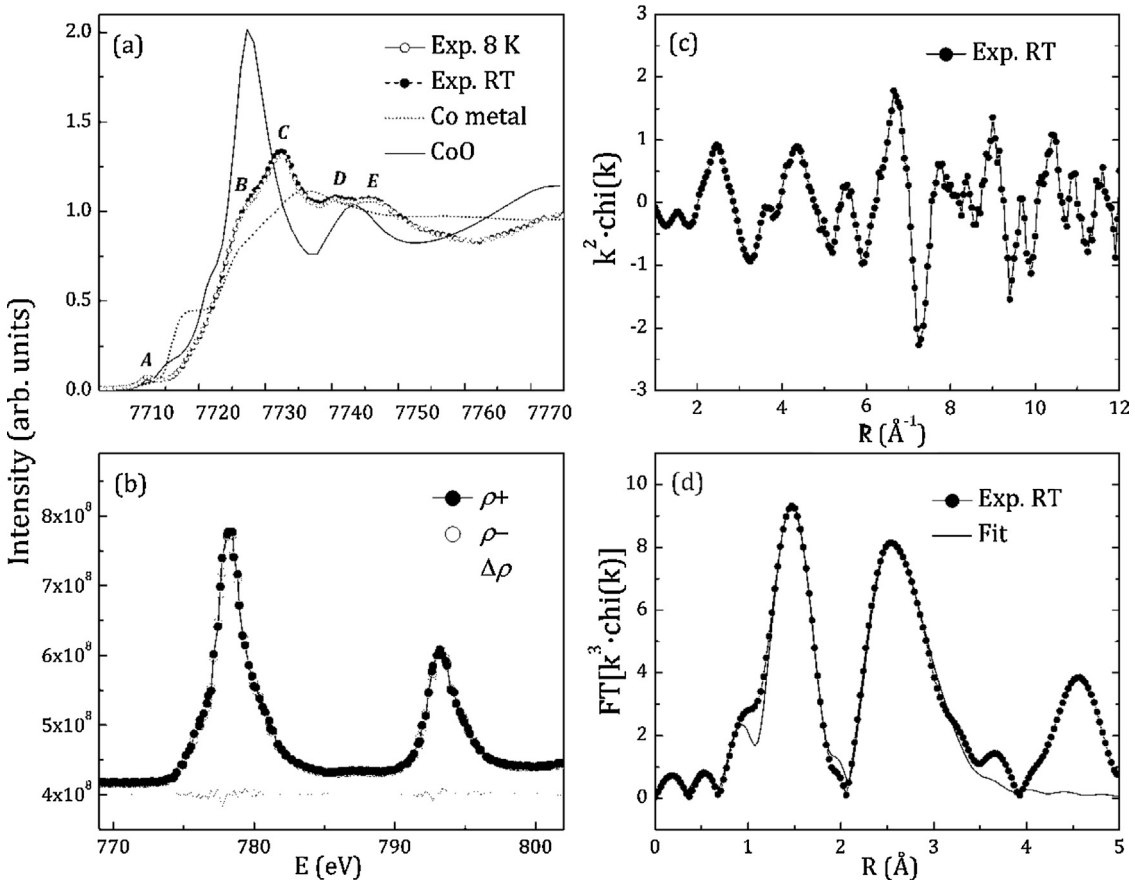

Fig. 3. (a) Experimental Co K-edge XANES spectra taken at 8 K (open circles) and RT (full circles) compared to theoretical spectra of metallic Co (dash–dot line) and CoO (full line); (b) Co $L_{2,3}$-edge XANES spectra taken at RT with right (ρ^+) and left (ρ^-) circularly polarized light and their difference $\Delta\rho = \rho^+ - \rho^-$ (XMCD); (c) Co K-edge EXAFS function taken at RT and (d) its Fourier transform (full circles) with theoretical fit (full line).

The behavior of the magnetization M(T) shown in Fig. 2d is typical for a paramagnet and obeys the Curie–Weiss law. Linear temperature dependence of the inverse magnetization (1/M) (see inset of Fig. 2d) confirms dominating paramagnetic contribution to the magnetic order. At low temperatures, the FM signal is completely overwhelmed by much stronger paramagnetic signal.

Fig. 3a shows experimental Co K-edge XANES spectra taken at 8 K and RT compared to theoretical spectra of metallic Co (dash–dot line) and CoO (full line). Markedly different shapes between the experimental and the model XANES spectra imply that neither Co clusters nor secondary CoO phase can be detected in the investigated sample. Characteristic features of the two experimental spectra (A–E) appear almost exactly alike. The only exception is slightly lower intensity of the main peak C (white line) at 8 K.

The Co K-edge XANES spectrum is determined by dipole transitions from 1 s to empty *p*-like states above the Fermi level and it is dominated by multiple-scattering (MS) events. PM $Zn_{1-x}Co_xO$ systems all share similar spectral shapes [33–37]. The pre-edge peak A results mainly from the 1s transitions to mixed Co 3d-O 2p and Co 4p-Co 3d states, feature B originates from the transitions to mixed sp-states, while the white line C and features D and E are predominantly due to 1 s → 4p transition [51]. The pre-edge in the XANES spectra of the investigated sample is indicative of Co^{2+} in local tetrahedral CoO_4 geometry [35]. Characteristic knee-like shape of the feature B was in [15] related to the presence of Co–O_v complexes aligned along *c*-axis and identified as a possible origin of the RTFM. Decrease in the white line (C) intensity at 8 K implies that there are less available empty Co *p*-states at low temperatures, which could be due the self diffusion of intrinsic defects [52], whose presence in the vicinity of Co could lead to larger charge transfer to Co. Feature D originates from MS contributions of the photoelectron backscattered from the nearest anion neighbors [51]. The feature D disappears when an O atom is missing from the second shell around the Co [51], which implies that the presence of the O_v in the second shell in the investigated sample most probably can be excluded.

Fig. 3b shows the RT Co $L_{2,3}$-edge XANES spectra taken with right (ρ^+) and left (ρ^-) circularly polarized light and their difference $\Delta\rho = \rho^+ - \rho^-$ (XMCD). The Co $L_{2,3}$ XANES spectrum results from 2p → 3d dipole transition and the L_3 and L_2 absorption lines are separated by approximately 15 eV due to spin-orbit splitting of the 2p core-hole. Negligible XMCD effect suggests that Co 3d-sublatice does not carry any significant magnetic moment, and that majority of Co ions are in paramagnetic state [2].

The Co K-edge EXAFS spectrum taken at RT is presented in Fig. 3c and its Fourier transform (FT) in Fig. 3d. The spectrum taken at 8 K is similar in appearance and therefore it was not shown. The EXAFS spectra are dominated by single-scattering events and the first FT peak (see Fig. 3d) arises from the photoelectrons backscattered from the first coordination oxygen shell. The mean distance between Co and O atoms (2.03(1) Å) derived from the EXAFS data analysis agrees well with the results reported for the samples with similar Co-doping level (1.977(5) [5]; 1.99(1) [22]; 2.00(1) Å [34]). However, the disorder parameter $\sigma^2 = 0.0013(7)$ Å^2 at 8 K and 0.0014(7) Å^2 at RT, is much smaller than previously reported ($\sigma^2 = 0.003(1)$ Å^2 [5]; $\sigma^2 = 0.0034(2)$ Å^2 [34]). These results imply that substitutional Co atoms are incorporated in ZnO

lattice at regular Zn atoms sites. Relatively small disorder induced by the Co-doping (which has been observed also by XRD) implies that Co^{2+} ions are in a high spin state with the tetrahedral covalent radius $R_C^{IV}(Co^{2+}) = 0.60$ Å comparable to $R_C^{IV}(Zn^{2+}) = 0.60$ Å [8]. The second peak in the FT spectrum (see Fig. 3d) is due to the photoelectrons backscattered from the second shell made of cations (Zn and Co). Metallic Co would result in a peak between the two ZnO peaks [35], which confirms that there has been no detectable Co-clustering in the investigated sample. However, from the Co K-edge EXAFS spectrum it is not possible to determine the exact composition of the second coordination shell [22], since Co and Zn have close atomic numbers and similar scattering amplitudes. Thus we cannot ascertain whether the distribution of Co ions is uniform.

Fig. 4a shows the O K-edge XANES spectra taken at 8 K with right (ρ^+) and left (ρ^-) circularly polarized light and their difference $\Delta\rho = \rho^+ - \rho^-$ (XMCD). Negligible XMCD signal indicates that in the investigated sample the O 2p-states are not magnetically polarized. Characteristic features (*a*–*d*) appearing in the experimental O K-edge XANES spectrum (see Fig. 4a) are very similar to those reported for FM $Zn_{1-x}Co_xO$ thin films [7], where the appearance of FM is related to formation of Co–O–Co chains. To examine possible connection of the structural defects with the absence of magnetism in the investigated sample, we performed theoretical calculations of the O K-edge absorption spectra of pure and Co-doped ZnO (Fig. 4b). Each particular defect (vacancy-O_v, Zn_v and interstitial-Co_i, Zn_i) is introduced in ZnO:Co constructed by replacing one of the first coordination Zn atoms by Co. In comparison to pure ZnO (see Fig. 4b) the O K-edge XANES spectrum of ZnO:Co exhibits richer structure and the whole spectrum is broader due to more dispersive O 2p-states [3,22]. Defects alter the O 1s binding energy and position of the conduction band bottom, which is manifested in shift of the XANES onset relative to the ZnO:Co. The pre-edge feature *a* (≈532 eV), absent in ZnO spectrum due to completely filled d-shell, has previously been ascribed to O 1s transitions to Co 3d-O 2p hybridized states [22], feature *b* (≈537 eV) to O 1s → O 2p transitions (with some contribution of mixed O 2p-Zn 4s states) [22,53], feature *c* (≈539 eV) to O 1s → O 2p-Zn 4p and feature *d* (≈543 eV) to O 1s → O 2p-Co 4p transition [22].

All spectral features (*a*–*d*) are reproduced in the ZnO:Co model spectra, but their intensities and energy position vary. It should be stressed that the pre-edge feature *a* appears only when the substitutional Co atom is in *c*-axis direction, which could be related to previously observed tendency of Co ions to cluster via O atoms along *c*-axis [22]. The feature *a* gains intensity from Co_i due to increased transition probability to Co 3d-O 2p hybridized states [3], but also in the presence of O_v and Zn_v. This implies that the pre-edge region of the XANES spectra also includes MS contribution from higher coordination shells. However, the presence of Co_i and O_v results in highly overestimated pre-edge intensity, which indicates that the tendency for Co–Co clustering and Co–O_v complexes formation in the investigated sample most likely can be excluded. The feature *b* is very much alike the pure ZnO spectrum and rises notably only in the presence of Zn_v, as a result of more available empty O 2p-states (lesser degree of O 2p-Zn 4s hybridization). The feature *c* is underestimated in all model spectra. The rise of *c*-intensity with Co doping [22], suggests that this region of the XANES spectrum involves MS contribution from Co-states from as high as third coordination shell around O. Model with Zn_i is much narrower with the features *c* and *d* merged together, and preserves the spectral shape also in the presence of Zn_v (model Zn_{vi}). Despite noticeable impact of each single point defect on the spectral shape (especially in the pre-edge region), none of them can be unambitiously associated with the absence of appreciable FM in the investigated sample. Even if the Co atoms are aligned along the *c*-axis as our results indicate, their clustering via O atoms would still be unlikely to stabilize the FM state due to AFM Co–O–Co coupling [20,54]. Weak FM response observed at room temperature could have originated from Zn vacancies, which are thought to be at the origin of FM in pure ZnO [12–14], but their amount obviously is not enough to induce substantial magnetic polarization of the O 2p-states, given the high structural perfection of the investigated sample. The later is in line with theoretical predictions of intrinsic PM in $Zn_{1-x}Co_xO$ with low density of defects [40,41].

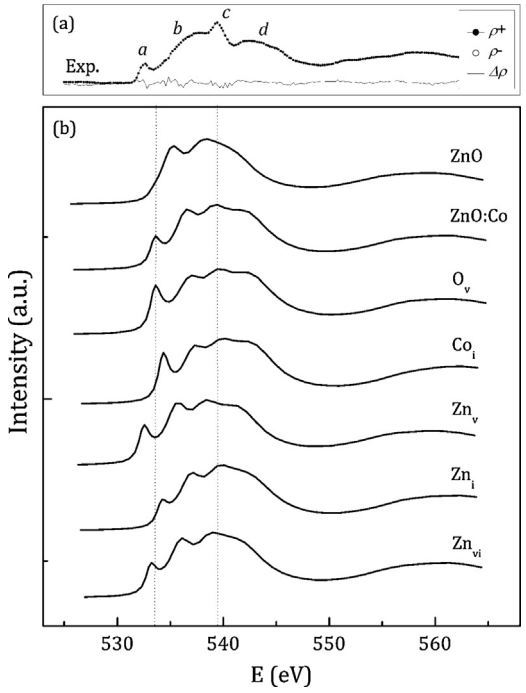

Fig. 4. (a) The O K-edge XANES spectra taken at 8 K with right (ρ^+) and left (ρ^-) circularly polarized light and their difference $\Delta\rho = \rho^+ - \rho^-$ (XMCD); (b) Theoretical O K-edge XANES spectra of ZnO and ZnO:Co system with a single point defect as indicated on the right (v—vacancy, i—interstitial). Vertical lines denote position of the most pronounced features *a* (pre-edge) and *c* (white line).

4. Conclusion

In conclusion, detailed investigations of $Zn_{0.95}Co_{0.05}O$ were carried out in order to better understand the magnetic properties and their correlation with the local and electronic structure. Obtained results reveal that the substitutional Co atoms are incorporated in ZnO lattice at regular Zn atomic sites and that the sample is characterized by high structural order. The Co^{2+} ions show no notable tendency for Co–Co clustering and Co–O_v complexes formation. Possible clustering of Co atoms via O atoms along the *c*-axis has not lead to stabilization of ferromagnetic order. There was no sign of magnetic polarization of O 2p-and Co 3d-states and the sample is paramagnetic at temperatures down to 5 K.

Acknowledgements

The research leading to these results has received funding from the European Community's Seventh Framework programme (FP7/

2007-2013) under the Grant agreement No. 226716 and is supported by Serbian Ministry of Education, Science and Technological Development under the Grant No. III 45012, the Program of scientific and technological cooperation between Republic of Serbia and Republic of Portugal under the Grant No. 451-03-02328/2012-14/03 and the Portuguese Research Grant Pest-OE/FIS/UI0068/2011 through FCT-MEC. The authors gratefully acknowledge HASYLAB @ DESY and ELETTRA for providing the beamtime. A1 and CiPo beamline scientists, in particular E. Welter (DESY) and N. Zema (ELETTRA), are acknowledged for the assistance during the XAFS/XMCD measurements.

References

[1] J.M.D. Coey, M. Venkatesan, C.B. Fitzgerald, Donor impurity band exchange in dilute ferromagnetic oxides, Nat. Mater. 4 (2005) 173–179.
[2] M. Kobayashi, Y. Ishida, J.L. Hwang, T. Mizokawa, A. Fujimori, K. Mamiya, J. Okamoto, Y. Takeda, T. Okane, Y. Saitoh, Y. Muramatsu, A. Tanaka, H. Saeki, H. Tabata, T. Kawai, Characterization of magnetic components in the diluted magnetic semiconductor $Zn_{1-x}Co_xO$ by x-ray magnetic circular dichroism, Phys. Rev. B 72 (2005) 201201–201204.
[3] A.P. Singh, R. Kumar, P. Thakur, N.B. Brookes, K.H. Chae, W.K. Choi, NEXAFS and XMCD studies of single-phase Co doped ZnO thin films, J. Phys.: Condens. Matter 21 (2009) 185005–185007.
[4] Z.H. Zhang, X. Wang, J.B. Xu, S. Muller, C. Ronning, Q. Li, Evidence of intrinsic ferromagnetism in individual dilute magnetic semiconducting nanostructures, Nat. Nanotechnol. 4 (2009) 523–527.
[5] S.-Y. Seo, E.-S. Jeong, C.-H. Kwak, C.-I. Park, Z. Jin, S.-H. Kim, S.-W. Han, X-ray absorption fine structure study of cobalt ion distribution in ferromagnetic $Zn_{1-x}Co_xO$ films, J. Phys.: Condens. Matter 25 (2013) 256005–256011.
[6] S. Francis, R. Saravanan, L.J. Berchmans, Effect of Co doping on the properties of ZnO bulk samples, J. Electron. Mater. 42 (2013) 701–710.
[7] S. Gautam, P. Thakur, P. Bazylewski, R. Bauer, A.P. Singh, J.Y. Kim, M. Subramanian, R. Jayavel, K. Asokan, K.H. Chae, G.S. Chang, Spectroscopic study of $Zn_{1-x}Co_xO$ thin films showing intrinsic ferromagnetism, Mater. Chem. Phys. 140 (2013) 130–134.
[8] S. Karamat, R.S. Rawat, P. Lee, T.L. Tan, S.V. Springham, R.V. Ramanujan, Synthesis and characterization of bulk cobalt-doped ZnO and their thin films, J. Supercond. Nov. Magn. 26 (2013) 3115–3123.
[9] A. Barla, G. Schmerber, E. Beaurepaire, A. Dinia, H. Bieber, S. Colis, F. Scheurer, J.-P. Kappler, P. Imperia, F. Nolting, F. Wilhelm, A. Rogalev, D. Müller, J.J. Grob, Paramagnetism of the Co sublattice in ferromagnetic $Zn_{1-x}Co_xO$ films, Phys. Rev. B 76 (2007) 125201–125205.
[10] Q. Wang, Q. Sun, G. Chen, Y. Kawazoe, P. Jena, Vacancy-induced magnetism in ZnO thin films and nanowires, Phys. Rev. B 77 (2008) 205411–205417.
[11] D. Gao, Z. Zhang, J. Fu, Y. Xu, J. Qi, D. Xue, Room temperature ferromagnetism of pure ZnO nanoparticles, J. Appl. Phys. 105 (2009) 113928–113934.
[12] X. Zuo, S.D. Yoon, A. Yang, W.-H. Duan, C. Vittoria, V.G. Harris, Ferromagnetism in pure wurtzite zinc oxide, J. Appl. Phys. 105 (2009) 07C508–3.
[13] X. Xu, C. Xu, J. Dai, J. Hu, F. Li, S. Zhang, Size dependence of defect-induced room temperature ferromagnetism in undoped ZnO nanoparticles, J. Phys. Chem. C 116 (2012) 8813–8818.
[14] C. Guglieri, E. Céspedes, A. Espinosa, M. Ángeles Laguna-Marco, N. Carmona, Y. Takeda, T. Okane, T. Nakamura, M. García—Hernandez, M.Á. García, J. Chaboy, Evidence of oxygen ferromagnetism in ZnO based materials, Adv. Funct. Mater. 24 (2014) 2094–2100.
[15] G. Ciatto, A. Di Trolio, E. Fonda, P. Alippi, A.M. Testa, A. Amore Bonapast, Evidence of cobalt-vacancy Complexes in $Zn_{1-x}Co_xO$ dilute magnetic semiconductors, Phys. Rev. Lett. 107 (2011) 127206–127215.
[16] T. Tietze, M. Gacic, G. Schütz, G. Jakob, S. Brück, E. Goering, XMCD studies on Co and Li doped ZnO magnetic semiconductors, New J. Phys. 10 (2008) 055009–055018.
[17] A. Pham, Y.B. Zhang, M.H.N. Assadi, A.B. Yu, S. Li, Ferromagnetism in ZnO:Co originating from a hydrogenated Co–O–Co complex, J. Phys.: Condens. Matter 25 (2013) 116002–116009.
[18] N. Khare, M.J. Kappers, M. Wei, M.G. Blamire, J.L. MacManus-Driscoll, Defect induced ferromagnetism in Co-doped ZnO, Adv. Mater. 18 (2006) 1449–1452.
[19] G.S. Chang, E.Z. Kurmaev, D.W. Boukhvalov, L.D. Finkelstein, S. Colis, T.M. Pedersen, A. Moewes, A. Dinia, Effect of Co and O defects on the magnetism in Co-doped ZnO: experiment and theory, Phys. Rev. B 75 (2007) 195215–195217.
[20] E.-C. Lee, K.J. Chang, Ferromagnetic versus antiferromagnetic interaction in Co-doped ZnO, Phys. Rev. B 69 (2004) 085205.
[21] B. Martínez, F. Sandiumenge, L. Balcells, J. Arbiol, F. Sibieude, C. Monty, Structure and magnetic properties of Co-doped ZnO nanoparticles, Phys. Rev. B 72 (2005) 165202–165208.
[22] Z. Sun, W. Yan, G. Zhang, H. Oyanagi, Z. Wu, Q. Liu, W. Wu, T. Shi, Z. Pan, P. Xu, S. Wei, Evidence of substitutional Co ion clusters in $Zn_{1-x}Co_xO$ dilute magnetic semiconductors, Phys. Rev. B 77 (2008) 245208–245216.
[23] S.-J. Hu, S.-S. Yan, M.-W. Zhao, L.-M. Mei, First–principles LDA + U calculations of the Co-doped ZnO magnetic semiconductor, Phys. Rev. B 73 (2006) 245205–245207.
[24] T. Dietl, T. Andrearczyk, A. Lipińska, M. Kiecana, M. Tay, Y. Wu, Origin of ferromagnetism in $Zn_{1-x}Co_xO$ from magnetization and spin-dependent magnetoresistance measurements, Phys. Rev. B 76 (2007) 155312–155315.
[25] J.M.D. Coey, J.T. Mlack, M. Venkatesan, P. Stamenov, Magnetization process in dilute magnetic oxides, IEEE T. Magn. 46 (2010) 2501–2503.
[26] Z.H. Wang, D.Y. Geng, S. Guo, W.J. Hu, Z.D. Zhang, Ferromagnetism and superparamagnetism of ZnCoO:H nanocrystals, Appl. Phys. Lett. 92 (2008) 242505–242603.
[27] M.P.F. de Godoy, A. Mesquita, W. Avansi, P.P. Neves, V.A. Chitta, W.B. Ferraz, M. A. Boselli, A.C.S. Sabioni, H.B. de Carvalho, Evidence of defect-mediated magnetic coupling on hydrogenated Co-doped ZnO, J. Alloy. Compd. 555 (2013) 315–319.
[28] Y. He, P. Sharma, K. Biswas, E.Z. Liu, N. Ohtsu, A. Inoue, Y. Inada, M. Nomura, J.S. Tse, S. Yin, J.Z. Jiang, Origin of ferromagnetism in ZnO codoped with Ga and Co: Experiment and theory, Phys. Rev. B 78 (2008) 155202–155207.
[29] M. Xu, H. Zhao, K. Ostrikov, M.Y. Duan, L.X. Xu, Effect of doping with Co and/or Cu on electronic structure and optical properties of ZnO, J. Appl. Phys. 105 (2009) 043708–043806.
[30] A.N. Andriotis, R.M. Sheetz, M. Menon, Defect-induced defect–mediated magnetism in ZnO and carbon-based materials, J. Phys.: Condens. Matter 22 (2010) 334210–334215.
[31] T. Thangeeswari, M. Priya, J. Velmurugan, Enhancement in the optical and magnetic properties of ZnO:Co implanted by Gd^{3+} nanoparticles, J. Mater. Sci.: Mater. Electron. 26 (2015) 2436–2444.
[32] I. Lorite, B. Straube, H. Ohldag, P. Kumar, M. Villafuerte, P. Esquinazi, C.E. Rodríguez Torres, S. Perez de Heluani, V.N. Antonov, L.V. Bekenov, A. Ernst, M. Hoffmann, S.K. Nayak, W.A. Adeagbo, G. Fischer, W. Hergert, Advances in methods to obtain and characterise room temperature magnetic ZnO, Appl. Phys. Lett. 106 (2015) 082406–082505.
[33] S. Yin, M.X. Xu, L. Yang, J.F. Liu, H. Rösner, H. Hahn, H. Gleiter, D. Schild, S. Doyle, T. Liu, T.D. Hu, E. Takayama-Muromachi, J.Z. Jiang, Absence of ferromagnetism in bulk polycrystalline $Zn_{0.9}Co_{0.1}O$, Phys. Rev. B 73 (2006) 224408–224415.
[34] T. Shi, S. Zhu, Z. Sun, S. Wei, W. Liu, Structures and magnetic properties of wurtzite $Zn_{1-x}Co_xO$ dilute magnetic semiconductor nanocomposites, Appl. Phys. Lett. 90 (2007) 102108–102113.
[35] T.C. Kaspar, T. Droubay, S.M. Heald, P. Nachimuthu, C.M. Wang, V. Shutthanandan, C.A. Johnson, D.R. Gamelin, S.A. Chambers, Lack of ferromagnetism in *n*-type cobalt-doped ZnO epitaxial thin films, New J. Phys. 10 (2008) 055010–055018.
[36] A. Ney, K. Ollefs, S. Ye, T. Kammermeier, V. Ney, T.C. Kaspar, S.A. Chambers, F. Wilhelm, A. Rogalev, Absence of intrinsic ferromagnetic interactions of isolated and paired Co dopant atoms in $Zn_{1-x}Co_xO$ with high structural perfection, Appl. Phys. Lett. 100 (2008) 157201–157204.
[37] H.B. de Carvalho, M.P.F. de Godoy, R.W.D. Paes, M. Mir, A. Ortiz de Zevallos, F. Iikawa, M.J.S.P. Brasil, V.A. Chitta, W.B. Ferraz, M.A. Boselli, A.C.S. Sabioni, Absence of ferromagnetic order in high quality bulk Co-doped ZnO samples, J. Appl. Phys. 108 (2010) 033914–033915.
[38] R. Bhargava, P.K. Sharma, S. Singh, M. Sahni, A.C. Pandey, N. Kumar, Switching in structural, optical, and magnetic properties of self-assembled Co-doped ZnO: effect of Co-concentration, J. Mater. Sci.: Mater. Electron. 25 (2014) 552–559.
[39] J. El Ghoul, M. Kraini, O.M. Lemine, L. El Mir, Sol–gel synthesis, structural, optical and magnetic properties of Co-doped ZnO nanoparticles, J. Mater. Sci.: Mater. Electron. 26 (2015) 2614–2621.
[40] G. Gu, G. Xiang, J. Luo, H. Ren, M. Lan, D. He, X. Zhang, Magnetism in transition-metal-doped ZnO: a first–principles study, J. Appl. Phys. 112 (2012) 023913–023915.
[41] S. Lardjane, G. Merad, N. Fenineche, A. Billard, H.I. Faraoun, Ab initio study of ZnCoO diluted magnetic semiconductor and its magnetic properties, J. Alloys Compd. 551 (2013) 306–311.
[42] M. Newville, IFEFFIT: Interactive XAFS analysis and FEFF fitting, J. Synchrotron Radiat. 8 (2001) 322–324.
[43] B. Ravel, M. Newville, ATHENA, ARTEMIS, HEPHAESTUS. Data analysis for X-ray absorption spectroscopy using IFEFFIT, J. Synchrotron Radiat. 12 (2005) 537–541.
[44] O.M.N.D. Teodoro, J.M.A.C. Silva, A.M.C. Moutinho, Multitechnique surface analysis system: apparatus description, Vacuum 46 (1995) 1205–1209.
[45] A.L. Ankudinov, B. Ravel, J.J. Rehr, S.D. Conradson, Real-space multiple-scattering calculation and interpretation of x-ray-absorption near-edge structure, Phys. Rev. B 58 (1998) 7565–7576.
[46] B. Ravel, ATOMS: crystallography for the X-ray absorption spectroscopist, J. Synchrotron Radiat. 8 (2001) 314–316.
[47] CRC Handbook of Tables for Applied Engineering Science, in: R.E. Bolz, G.L. Tuve (Eds.), CRC, Press, Boca Raton, Florida, 1973.
[48] M.C. Biesinger, B.P. Payne, A.P. Grosvenor, L.W.M. Lau, A.R. Gerson, R. St.C. Smart, Resolving surface chemical states in XPS analysis of first row transition metals, oxides and hydroxides: Cr, Mn, Fe, Co and Ni, Appl. Surf. Sci. 257 (2011) 2717–2730.
[49] G.A. Carson, M.H. Nassir, M.A. Langell, Epitaxial growth of Co_3O_3 on CoO (1 0 0), J. Vac. Sci. Technol. A 14 (1996) 1637–1642.
[50] C.D. Wagner, W.M. Riggs, L.E. Davis, J.F. Moulder, Handbook of X-ray Photoelectron Spectroscopy, PerkinElmer Corp., USA, 1979.

[51] S. Zhang, L. Zhang, H. Li, J. Li, Z. Jiang, W. Chu, Y. Huang, J. Wang, Z. Wu, Investigation of annealing-induced oxygen vacancies in the Co-doped ZnO system by Co K-edge XANES spectroscopy, J. Synchrotron Radiat. 17 (2010) 600–605.
[52] P. Erhart, K. Albe, Diffusion of zinc vacancies and interstitials in zinc oxide, Appl. Phys, Lett. 88 (2006) 201918–202013.
[53] J.-H. Guo, L. Vayssieres, C. Persson, R. Ahuja, B. Johansson, J. Nordgren, Polarization-dependent soft-x-ray absorption of highly oriented ZnO microrod arrays, J. Phys.: Condens. Matter 14 (2002) 6969–6974.
[54] Y. Zhang, M.H.N. Assadi, S. Li, Giant stability of substituent Co chains in ZnO:Co dilute magnetic oxides, AIP Adv. 2 (2012) 042155–042156.